Chapter 2

STABLE GLASS SEALS FOR INTERMEDIATE TEMPERATURE (IT) SOFC APPLICATIONS

Qingshan Zhu, Lian Peng, and Tao Zhang
Multiphase Reaction Laboratory, Institute of Process Engineering, Chinese Academy of Sciences, Beijing 100080, China

INTRODUCTION

Solid oxide fuel cells (SOFCs), which convert chemical energy of incoming fuels to electricity via electrochemical reactions, have become increasingly attractive to the utility and automotive industries for a number of reasons, including their high efficiency and low emissions [1]. Among different types of SOFCs, planar SOFC designs have several advantages over tubular designs [2], such as easier to be manufactured, lower processing cost, shorter current paths, and consequently higher power densities, etc. Planar SOFCs have therefore been extensively investigated over the past decade. In the planar design, a gas-tight seal is required to keep the fuel gas and air separated from each other to prevent direct combustion which decreases power generation efficiency and causes local overheating. The seals must be stable in both oxidized and reduced atmospheres, be chemically compatible with other fuel cell components, and have matched thermal expansion coefficients (TEC) with other components. Moreover, these properties must be kept unchanged over the required lifetime of at least 40,000 h at elevated temperatures, together with hundreds of thermal cycles. Although many advances have been achieved for SOFC sealing, none of the current sealing materials can meet all the above criteria at the same time. Accordingly, sealing has been identified as one of the toughest technical challenges for the development of planar SOFCs [3].

In the present chapter, we will begin with a brief review of the state-of-the-art sealing concepts and sealing materials, followed by identifying the major problems for glass-based sealing materials. Then our new approach for sealing glass development will be introduced. Finally, the TEC, chemical compatibility with 8YSZ (8 mol% yttria stabilized zirconia) and thermal stability of the newly developed sealing glasses will be discussed in detail.

STATE-OF-THE-ART SOFC SEALING

Over the past decade, different SOFC sealing concepts have been proposed. Among these sealing concepts, rigid bonded sealing and compressive sealing have been extensively investigated [4], together with the development of suitable materials.

Rigid Sealing

Rigid sealing refers to the concept that SOFC components are rigidly bonded together by sealants, where after sealing the bonded components cannot move against each other. Two types of materials, glass-based and alloy-based (braze) materials, have been investigated for this sealing concept. The status quo of these two types of sealing materials will be summarized below.

Glass/Glass–Ceramic Sealants

Glass or glass–ceramic materials are the most commonly used sealants for SOFCs because the properties can be easily tailored by manipulating glass compositions, and also because glasses are cost effective and simple to be processed. Glasses are typically distinguished by the glass formers, like phosphate glasses, borate glasses, and silicate glasses. All the three types of glasses have been explored for SOFC sealing. It has been generally showed that at high temperatures, glasses purely based on phosphate are easily volatilized and tend to react with the Ni-YSZ anode to form nickel phosphate and zirconiumoxyphosphate [5,6]. Also, phosphate glasses usually crystallize to form meta- or pyrophosphates, which exhibit low stability in a humidified fuel gas at SOFC operating temperatures. Consequently, glasses purely based on phosphate are not suitable for SOFC sealing applications [7]. Borate-based glasses and glass–ceramics have also been investigated as SOFC sealing materials. The problem for glasses with boron oxide as the only glass former lies in the fact that borate tends to react with a humidified fuel atmosphere to form volatile species like $B_2(OH)_2$ and $B_2(OH)_3$ at SOFC operating temperatures, which causes loss of the glass seal [8]. It has been shown that a borate based glass exhibited a weight loss up to 20 wt% in a wet fuel atmosphere [5] and extensive interactions with other cell components both in air and wet fuel gas. Silicate glasses are most attractive as potential sealing materials because these glasses have much better chemical compatibility and stability as compared with phosphate- and borate-based glasses. Most sealing glass R&Ds were therefore focused on silicate glasses and glass–ceramics. Some

typical glass and glass–ceramic seals reported in literature [7–13] are summarized in Table 2-1.

Among various properties, glass transition temperature (T_g) and TEC are most extensively investigated, as these two properties directly determined sealability of a glass. T_g is the temperature where the transition of a material from the solid state into the liquid state takes place. T_g is often determined via dilatometry and roughly corresponds to a viscosity of ~10^{12} Pa s, below which the material is "soft" enough to release thermal stress through plastic deformation. So, the T_g is the indicator of the "softness" of a glass. For SOFC applications, it is desirable that the T_g be as low as possible since significant thermal stress only starts to build up below the T_g. On the other hand, the sealant viscosity at fuel cell operating temperatures must be greater than 10^3 Pa s, below which the sealant would flow readily, to provide sufficient sealing strength [14]. So, a suitable sealing glass and glass–ceramic should flow sufficiently to provide an

Table 2-1. Compositions of glass/glass–ceramic sealants (mol%)

Glass former	Al_2O_3	Others	T_g (°C)	TEC (10^{-6} K^{-1})	Ref.
$52P_2O_5$	16	32MgO	–	–	[7]
$5SiO_2 - 50P_2O_5$	15	30MgO	–	–	
$18SiO_2 - 43P_2O_5$	13	26MgO	–	–	
$30SiO_2 - 37P_2O_5$	11	22MgO	–	–	
$8.11SiO_2 - 40.29B_2O_3$	6.92	$24.6SrO–20.1La_2O_3$	740–780	11.5	[8]
$5.72SiO_2 - 46.04B_2O_3$	17.69	$26.8SrO–3.75La_2O_3$	560	9.69	
$11.23SiO_2 - 27.01B_2O_3$	16.27	$41.76SrO–3.74La_2O_3$	700	9.2	
$28.29SiO_2 - 18.5B_2O_3$	14.26	$35.31SrO–3.65La_2O_3$	740–750	8.08	
$34.4SiO_2 - 17.2B_2O_3$	10.3	$36.1BaO–2La_2O_3$	627	10.1	[9]
$33.3SiO_2 - 16.7B_2O_3$	10	$35BaO–5La_2O_3$	656	11.1	
$33.3SiO_2 - 16.7B_2O_3$	10	$35BaO–5ZrO_2$	655	9.3	
$30.1SiO_2 - 21.5B_2O_3$	10.3	$36.1BaO–2ZrO_2$	614	10.6	
$34.4SiO_2 - 17.2B_2O_3$	10.3	36.1BaO–2NiO	620	11.5	
$33.3SiO_2 - 16.7B_2O_3$	10	35BaO–5NiO	615	12.8	
$50.5P_2O_5 - 11.3B_2O_3$	12.6	25.6MgO	603	5.9	[10]
$50.5P_2O_5 - 11.3B_2O_3$	12.6	$25.6CaO–5.0Cr_2O_3$	605	7.9	
$46.5P_2O_5 - 11.3B_2O_3$	11.6	25.6MgO+5.0CaO	618	5.7	
$42.5P_2O_5 - 11.3B_2O_3$	10.6	$25.6MgO–5.0Cr_2O_3$	620	5.9	
$21.45SiO_2 - 6.66B_2O_3$	5.39	56.1BaO–7.1CaO	–	–	[11]
$50SiO_2 - 14B_2O_3$	11	$24BaO–0.5As_2O_3$	–	–	[12]
$47.5SiO_2 - 13.3B_2O_3$	10.4	$22.8BaO–5MgO–0.5As_2O_3$			
$45SiO_2 - 22.6B_2O_3$	9.8	$21.6BaO–10MgO–0.5As_2O_3$	–	–	
$60SiO_2$		32BaO–8MgO	703	9.8	[13]
$60SiO_2$		32BaO–8ZnO	670	10.5	
$50SiO_2$		40BaO–10MgO	686	12	
$50SiO_2$		40BaO–10ZnO	676	11.5	

adequate seal and to release the thermal stress as much as possible, while maintaining sufficient rigidity to achieve mechanical integrity. T_g of a glass would decrease with increasing the contents of boron oxide, alkali metal oxides as well as alkaline earth metal oxides.

The TEC is another important criterion for the selection of sealing glasses and glass–ceramics as TEC mismatch is the origin of thermal stress. TEC values are in the range of $10.5–12.5 \times 10^{-6}$ K^{-1} (room temperature to 800°C) for SOFC components (anodes, 8YSZ electrolyte, cathodes, interconnects), so it is generally required that the TEC of sealants should be also in the range of $10.5–12.5 \times 10^{-6}$ K^{-1}. Normal silicate glasses usually have much lower TEC values and it is not easy to obtain a glass of high TEC values together with suitable T_g. The TEC of silicate glasses will normally increase with increasing alkali metal oxides contents. However, Li^+, Na^+, and K^+ cations are easily diffused into other fuel cell components, which cause cell performance degradation. Consequently, alkali metal oxides addition is not recommended in most cases [14]. To achieve high TEC values, alkaline earth metal oxides are often used [9], among which BaO addition is most attractive due to its relatively large contribution to the TEC increase among all alkaline earth metal oxides. Another way to increase sealants' TEC is through deliberate crystallization control of a glass to form a glass–ceramic. Glasses are not thermodynamically stable and tend to crystallize at SOFC operating temperatures. However, uncontrolled crystallization usually results in unwanted phases that might have too low or too high TECs. The crystallization is a thermodynamically favorable and kinetically controlled process. To obtain suitable crystalline phases, it often needs to add nucleating agents to induce the nucleation of certain phases. Also, crystallization kinetics, like nucleating temperature and time, crystallization temperature and time, is critical to the property control. It has been shown that the formation of Ca_2SiO_4, $BaSiO_3$, $BaSi_2O_5$, and $Ba_3CaSi_2O_8$ phases would increase the TEC as these phases have high TECs, while phases like hexacelsian ($BaAl_2Si_2O_8$), celsian, and cordierite ($Mg_2Al_4Si_5O_{18}$) can significantly decrease the TEC [4].

Glass-based sealants must be chemically stable in both air and fuel gas atmospheres throughout the service time of SOFC. For the phosphate glasses and borate-based glasses, it has been shown that the stability is insufficient even for a short time of exposure, especially in wet fuel atmospheres. However, chemical stability for silicate glasses is seldom reported and needs to be further investigated. The sealants must be chemically compatible with other fuel cell components. Investigations showed that the chemical compatibility of glass–ceramic sealants with the 8YSZ electrolyte was generally good, while severe reactions were commonly observed between glass-based sealants and metal interconnects. The

sealant–interconnect interaction is problematic because such reactions cause changes in both glass phase and the interconnect phase around the interface. It has been demonstrated that small composition variation of glasses or metals could result in significant difference in interface composition and structure [15]. For example, investigations revealed that small amounts (<0.5 wt%) of Al, Si, Mn, and Ti in the interconnect metals have great influence on the interaction rate. It had also been shown that pores up to several hundred micrometers were observed after only a few hours contact of SUS 430 with a sealing glass at 750–800°C [11]. The interaction mechanism among different metals and glasses has not yet been fully understood and needs further efforts to get a profound understanding about these interactions.

Thermal stability is another very important property for glass-based sealants since seals need to function for at least 40,000 h. As mentioned previously, glasses are thermodynamically unstable and have the tendency to transform to thermodynamically stable phases through crystallization during exposure at SOFC operating temperatures. The transformation is accompanied with thermal property changes, which might enlarge the TEC mismatch between the sealant and the materials being sealed. For example, the TEC value decreased up to 36% for a glass after being heat treated at 800°C for 1,000 h [9].

Brazes

The other approach to a rigid seal is a metallic braze. Metallic materials have lower stiffness as compared to ceramics and can undergo plastic deformation more easily, both of which allow for accommodation of thermal and mechanical stresses. Brazes are often based on alloys of Pt, Au, Ag, Pd, Cu, Ni, Ti, and Cr. Of these, precious metal-based alloys are most promising for use in SOFCs, as these brazes are capable of withstanding fuel and oxidizing atmospheres at high temperatures [16]. One of the major problems in obtaining a good metal-ceramic sealing is inadequate wetting of the ceramic by braze metals. Approaches employed to solve the problem include the addition of reactive elements like Ti, Hf, Zr, etc. and the addition of metal oxides such as CuO, Al_2O_3, Al_2TiO_5, etc. [17]. The addition of metal oxides could also be used as a mean to adjust the TEC of brazes, as the TECs of most brazes are in the range of 16–21 $\times 10^{-6}$ K^{-1}, which are much higher than those of 8YSZ and other SOFC components. However, brazes are electrically conductive, so proper insulation should be achieved to avoid short-circuit when applied to SOFCs. Brazes also have insufficient long-term oxidation resistance at high temperature under SOFC atmospheres.

Compressive Seals

Another possible alternative to glass-based seals is the use of compressive, nonbonding seals. If the seals are nonbonding, the individual stack components are free to expand and contract during thermal cycling. Compressive seals utilize materials such as sheet-structure silicates, which do not bond to the SOFC components; instead, hermeticity is achieved by applying a compressive force to the stack, using suitable sealing materials as the gasket. The use of compressive seals brings several new challenges to SOFC stack design, like a load frame must be included to maintain the desired level of compressive load during operation, and the stack components must be able to withstand the compressive load required for adequate sealing for the lifetime of the stack. Compressive seal materials are mostly two types of materials: metallic materials and mica-based materials [18]. As mentioned before, metallic materials are seldom reported due to their electric conductivity. The research in this area was mainly focused on mica-based materials.

Micas belong to a class of minerals known as phyllosilicates, and are composed of sheets of silicate tetrahedrons. They are generally known for their high resistivity and uniform dielectric constant/capacitance stability, and consequently are used extensively in electronic devices [19]. Micas can accommodate large thermal stress because they do not bond to the SOFC components. However, mica seals alone normally exhibit high leak rates several orders of magnitudes than those of glass-based seals [20]. It is therefore necessary to combine with other materials to reduce the leak rate to an acceptable level for SOFC applications. Silver and glass were commonly used as the composite materials to improve the hermeticity of mica seals. Figure 2-1 shows the effect of various interlayers on the leak rate (sccm cm^{-1}, i.e., standard cubic centimeter per minute per unit leak length of seal) [21]. Clearly, the use of a glass as the interlayer for hybrid mica seals is more effective than silver interlayer in blocking or filling the surface defects such as grooves and voids presented at these interfaces. Moreover, leak rate decreases with increasing compressive stress.

Although the combination of glass with mica was found to be attractive, mica seals were also faced on many challenges. In general, seals with elastic or plastic properties require a permanent compression load to achieve gas tightness. In most cases, the sealing load is higher than that required for electrical contact between electrodes and interconnects, so an adaptation of the stack design to the requirements of a compressive seal is a prerequisite for application of this concept.

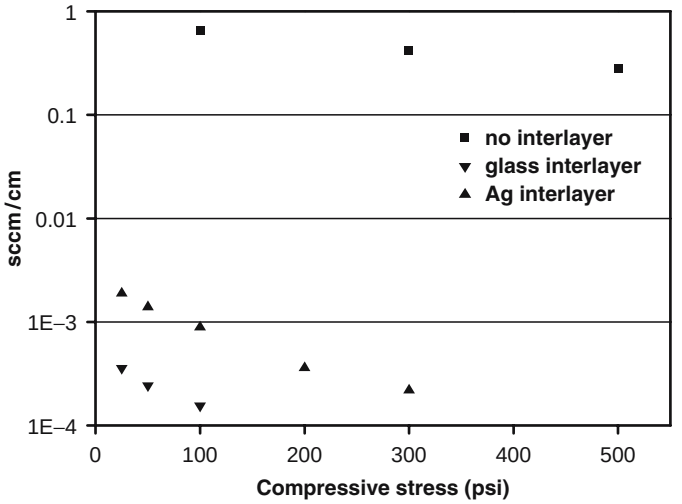

Figure 2-1. Effect of the applied compressive stress on the normalized leak rate of muscovite single-crystal mica with and without interlayer at 800°C

Challenges for Glass-Based Sealants

Due to the extremely stringent requirements for the sealing material, e.g., seal materials should be stable and capable of a service life of more than 40,000 h and hundreds of thermal cycles for stationary systems, or at least 5,000 h and 3,000 thermal cycles for transportation systems, the fundamental difficulty in fabricating planar SOFCs is how to effectively seal the anode/electrolyte/cathode assembly together with the interconnect to create a hermetic and stable stack. Glass or glass–ceramic materials are the most commonly used sealants for SOFCs. Although many advances have been achieved for glass-based seals, several challenges remain unsolved. Firstly, glass-based seals have very poor thermal stability, where the thermal properties of glass based seals change continuously with the time of exposure at high temperatures. As previously mentioned, glasses are easily crystallized at SOFC operating temperatures, which might cause a significant change about the thermal expansion coefficient. As demonstrated by Sohn et al. [9], the TEC change can be more than 36% after being kept at 800°C for 1,000 h. The change of the TEC value and other thermal properties can induce significant thermal stress at the sealing interface, and will ultimately cause the failure of the sealing as well as the stack when the thermal stress reaches a critical point. So, the thermal

stability of current state of the art sealing glass/glass–ceramics needs to be further improved. Secondly, glass-based seals often have poor chemical compatibility with other SOFC components (especially with interconnects) at operation temperatures. As demonstrated by Yang et al. [11], extensive reactions with $BaCrO_4$ as the main resultant product were observed between a glass-based seal and metal alloys, where the reactions generated pores up to 200 μm aligned along the metal–glass interface. In some cases, the reaction also caused separation of the glass with the alloy matrix, possibly due to the thermal expansion mismatch between $BaCrO_4$ and metal interconnect. The extensive formation of interfacial pores and interface separation will greatly reduce interfacial bonding strength, which would be detrimental to structural stability of the SOFC stacks. Therefore, glass-based seals with much better thermal stability and chemical compatibility are still needed to be developed.

APPROACH FOR SEALING GLASS DEVELOPMENT

Conventionally, glasses were developed using the "trial and error" approach. However, such an approach does not work effectively for sealing glass development as sealing glasses usually have quite complex compositions and have to meet several requirements, such as TEC match, suitable viscosity, chemical compatibility with other materials, chemical stability under fuel cell atmospheres, long-term thermal stability, etc. For such complex composition and multiobjective glass development, it is already difficult enough to find a composition that could meet all the requirements, and it is even more difficult to optimize the composition to fit each requirement using the "trial and error" approach, which might be the primary reason for the slow advancement of glass-based seals over the past decade. A new approach, capable of quantitative design of sealing glasses, would be beneficial to speeding up the sealing glass development and to accelerating the commercialization of SOFCs as well.

In the present study, a new approach, aiming at quasiquantitative design of the chemical compatibility, chemical stability, TEC, and viscosity for sealing glasses, has therefore been proposed. As illustrated in Figure 2-2, a combined model, coupled from the TEC model and the viscosity model [22], will be first established. A glass composition could then be designed to meet the TEC and viscosity requirements. In the meantime, a thermodynamic model will also be constructed for predicting various reactions between a glass and other materials (anode, electrolyte, cathode, etc.). The glass composition from the combined model would then be used as the input for the thermodynamic investigation to check the chemical

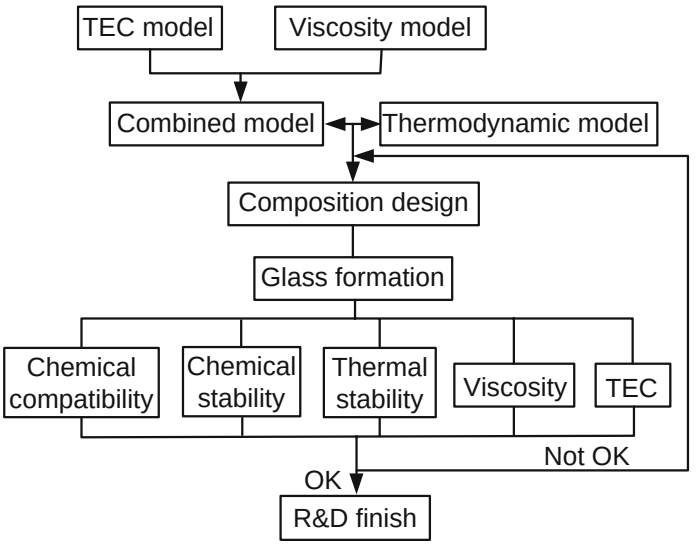

Figure 2-2. A schematic procedure for sealing glass development

compatibility between the glass and other materials, and the composition would be adjusted according to the results from thermodynamic analyses. The composition would then be redesigned using the combined model, taking the composition from the thermodynamic analyses as the constraint. Through the simulation between the combined model and the thermodynamic model, a composition that could meet all the requirements may hopefully be obtained. A glass will be made according to the composition, and its properties, including chemical compatibility with other materials, thermal stability, viscosity and TEC, etc., will be experimentally checked to validate the composition design. If any of the properties failed to meet the requirements, the glass design would start from the beginning again, taking into account the information obtained from the validation experiments.

The TEC of a glass is normally predicted by the weighted model as expressed by (1):

$$\alpha = \sum_i \alpha_i c_i, \tag{1}$$

where α is the TEC of the glass (10^{-6} K^{-1}), α_i is the TEC contribution factor of the ith component (10^{-6} K^{-1}) and c_i is the mole fraction of the ith component in the glass. Some TEC contribution values of common oxides are listed in Table 2-2. The viscosity of glasses against temperature and

Table 2-2. TEC contribution factors for various metal oxides [22]

Substance	α_i (10^{-6} K^{-1})	Substance	α_i (10^{-6} K^{-1})
SiO_2	0.005 – 0.038	B_2O_3	–0.050 to 0.00
Li_2O	0.270	SrO	0.160
Na_2O	0.395	BaO	0.200
K_2O	0.465	PbO	0.130 to 0.190
MgO	0.060	Al_2O_3	–0.030
CaO	0.130	ZrO_2	–0.060
ZnO	0.050	P_2O_5	0.140
MnO	0.105	Fe_2O_3	0.055
CoO	0.050	NiO	0.050
SnO_2	–0.045	TiO_2	–0.015 to 0.03
CuO	0.030	Ga_2O_3	–0.020

composition is normally expressed by the so-called Vogel–Fulcher–Tammann (VFT) equation as:

$$\log \eta = -A + B/(T - T_0). \tag{2}$$

Investigations by Lakatos et al. [22,23] demonstrated that the constants A, B, and T_0 can be well represented by simply additive terms for a certain range of compositions close to those used for containers and flat glasses as:

$$A = 1.713 + \Sigma a_i c_i, \tag{3}$$

$$B = 6237.01 + \Sigma b_i c_i, \tag{4}$$

$$T_0 = 149.4 + \Sigma t_i c_i, \tag{5}$$

where a_i, b_i, t_i are the VFT coefficients for the ith component and c_i is the concentration of the ith components in a glass.

Our investigations showed that the viscosity model and the TEC model could be easily combined together using a weighted sum strategy after normalization of the TEC data and the viscosity data, and it was quite easy to obtain a glass composition that meets the targeted values for both the viscosity and TEC models using an optimization algorithm [24]. The problem for the glass composition design using the combined model however lies in the fact that these two models are only valid for a certain range of compositions and the prediction accuracy is thus questionable for compositions out of the range. Investigations revealed that the prediction accuracy for these two models was actually very poor for glasses relevant to SOFC seals. For example, for the glass of $30.1SiO_2$–$21.5B_2O_3$–36.$1BaO$–$10.3Al_2O_3$– $5.0ZrO_2$ composition (mol%), the TEC model predicts a TEC value of 7.0×10^{-6} K^{-1}, whereas the TEC was measured to be

10.6×10^{-6} K^{-1} [9] (room temperature to 700°C), indicating that the coefficients in Table 2-2 are not completely applicable to this composition. It is therefore necessary to amend the coefficients for both the viscosity model and the TEC model in order to make them applicable to those compositions relevant to SOFC glass seals.

The chemical compatibility of a glass with other materials and chemical stability of a glass can be investigated by thermodynamic investigations. While $\Delta G < 0$ could be used to judge whether a reaction could proceed for simple systems, reactions occurred in complex systems like sealing glass would normally be simulated using minimizing the free energy method [25] as indicated by (6) and (7).

$$\text{Min: } G = \sum_{j=1}^{M} \sum_{i=1}^{N_j} n_i \mu_i, \tag{6}$$

$$\text{Conservation of Mass: } \sum_{j=1}^{M} \sum_{i=1}^{N_j} a_{ik} n_i = B_k \quad (k = 1, 2, \ldots, NN), \tag{7}$$

where G is the total free energy of the system, M is the total phases in the system, n_i is the molar quantity of the ith substance in a specified phase, N_j is the total number of substances in the jth phase, μ_i is the chemical potential of the ith substance under the specified condition, NN is the number of elements in the system, a_{ik} is the molar quantity of the kth element in the ith substance in a specified phase and B_k is the total molar quantity of the kth element in the system. The μ_i is expressed differently for gas phase, liquid phase and pure condense phase by (8), (9) and (10), respectively.

$$\mu_i = \mu_i^0 + RT \ln f_i, \tag{8}$$

$$\mu_i = \mu_i^0 + RT \ln a_i, \tag{9}$$

$$\mu_i = \mu_i^0, \tag{10}$$

where μ_i^0 is the chemical potential of the ith substance under the standard state, f_i is the fugacity of the ith gas species and is equal to partial pressure p_i for an ideal gas, a_i is the activity of ith liquid species and is equivalent to the mole fraction x_i for an ideal solution, R is the universal gas constant, and T is gas temperature in Kelvin.

The accuracy of thermodynamic simulation is dependent on thermodynamic model. It is quite easy to model the gas phase and the pure condense phases, while the liquid solution of oxide glasses have been difficult to model because of strong interactions between constituents, and it has been found that simple solution models do not accurately reproduce

the thermodynamic and phase relations in most oxide liquid systems [26]. In the past two decades two approaches, the modified quasichemical model by Pelton et al. [27,28] and the modified associate species model by Spear et al. [29], were proposed for the simulation of oxide melts. The modified associate species model is attractive because it has been demonstrated that it can accurately represent the thermodynamic behavior of some complex chemical systems over wide temperature and composition ranges [26]. The basis for the modified associate species approach is that the complex oxide solutions can be represented by an ideal solution of end-member species and intermediate associate species. The intermediate associate species can be fictive species whose thermodynamic data can be determined by a reconstruction of an experimentally determined phase diagram through an optimization process.

To simulate a glass system relevant to our sealing glass development, the SiO_2–B_2O_3–BaO–CaO–Li_2O–ZrO_2 system was tentatively modeled using the associate species approach, where the model consists of 22 gas species including O_2, N_2, NO, NO_2, B_2O(g), B_2O_2(g), AlO(g), Al_2O(g), AlO_2(g), Al_2O_2(g), B_2O_3(g), CaO(g), SiO(g), $AlBO_2$(g), ZrO_2(g), ZrO(g), ZrN(g), La_2O_2(g), La_2O(g), BaO(g), Ba_2O(g), Ba_2O_2(g); and 19 pure solid phases including B_2O_3(cr), CaO(cr), Al_2O_3(cr), SiO_2(cr), CaB_4O_7(cr), Al_2SiO_5(cr), $CaAl_2SiO_6$(cr), ZrO_2(cr), $ZrSiO_4$(cr), $CaZrO_3$(cr), ZrN(cr), ZrB_2(cr), $BaZrO_3$(cr), Ba_2ZrO_4(cr), $Y_2Zr_2O_7$(cr), La_2O_3(cr), Y_2O_3(cr), BaO(cr), BaO_2(cr). For the liquid phase, apart from the end member species of B_2O_3(l), CaO(l), Al_2O_3(l), SiO_2(l), Li_2O (l), ZrO_2(l), CaO(l), BaO(l), seven associate species of $CaSiO_3$(l), $Al_4B_2O_9$(l), CaB_4O_7(l), Ba_2ZrO_4(1), $Al_2Si_2O_7$(l), $Li_2B_4O_7$(l), $LiBO_2$(l), $LiAlSi_2O_6$(l) were included. Thermodynamic data for the end members and the associate species were taken from references [30,31], no attempts were made to evaluate more associate species according to various phase-diagram at this stage. Gibbs free energy of Ba_2ZrO_4(cr) were estimated by the regular solution model. The thermodynamic model was used to predict chemical compatibility of various glasses with 8YSZ at high temperatures (at least above the liquid temperature of glasses) during the glass development.

EXPERIMENTAL

Glass Preparation

Glasses were prepared from reagent-grade Al_2O_3, SiO_2, B_2O_3, La_2O_3, ZrO_2, Y_2O_3, $BaCO_3$, $CaCO_3$, and $MgCO_3$. The oxides and carbonates in prescribed composition were melted in a Pt crucible at 1,250–1,400°C

in air for 2–4 h, followed by quenching the glass melt in water. The as-quenched glass was remelted at 900–1,000°C for 0.5 h and cooled to room temperature naturally to obtain a glass block. The glass block was then cut and ground into bars with nominal dimensions of $15 \times 4 \times 2$ mm^3 for various characterizations.

Heat Treatment

Heat treatments were performed for the as-prepared glasses to obtain glass–ceramics. Nucleating agents, including ZrO_2, TiO_2, Cr_2O_3, P_2O_5 were added up to 5 wt% to their parent glasses through comelting with the parent glasses. The heat treatment procedure was determined based on glass transition temperature (T_g), crystallization temperature (T_c) and liquid temperature (T_{liq}) of glasses, which were determined by differential thermal analyses (DSC-TG, Netzsch STA 449C, Germany). In a typical experiment, after melting a glass together with a proper amount of a nucleating agent, the glass was first heated at a heating rate of 10°C min^{-1} to ~690°C for 0.5–2 h to achieve homogenous initiation of crystallization, then to a temperature between T_c and T_{liq} for 2–10 h to obtain a glass–ceramic, followed by cooling down to room temperature at a cooling rate of 10°C min^{-1}. The as heat-treated glass was then subjected to various characterizations to reveal the nature of the as-obtained crystals.

Glasses and Glass–Ceramics Characterization

All the as-prepared glasses were characterized by X-ray diffractometry (XRD, X'Pert MPD Pro, PANalytical, The Netherlands) to check whether the glasses are amorphous. Thermal properties of the glasses, such as the glass transition temperature (T_g), softening temperature (T_s), crystallization temperature (T_c) and liquid temperature (T_{liq}), were measured using differential thermal analyses for both glasses and glass–ceramics. TECs of glasses and glass–ceramics were determined in stagnant air from room temperature to T_g via dilatometry (L75/1550, LINSEIS, Germany) at a heating rate of 10°C min^{-1}. A total of six specimens were measured for the TEC and the average value was used as the TEC value for a glass. The TEC of 8YSZ was also characterized for the purpose of comparison. The glass–ceramics were characterized by XRD to reveal the precipitated crystalline phases. The wetting behavior of the parent glass on 8YSZ (8 mol% yttria stabilized zirconia) was examined by observing the shape change of a glass pellet with the dimension of $5 \times 5 \times 1$ mm^3 under a home-assembled high temperature microscope, where the glass pellet was put on the top of a 8YSZ plate and continuously heated

to 900°C at a heating rate of 5°C min^{-1}. The shape change was recorded using a digital camera connected to the microscope, where pictures were taken at an interval of 10°C.

Long-Term Thermal Stability and Chemical Compatibility

Thermal stability of the as-prepared glasses was investigated through heat treatment at 700°C for up to 500 h. Glasses were first heated to 920°C for 30 min in a Pt crucible with a heating rate of 5°C min^{-1}. They were then cooled with a cooling rate of 5°C min^{-1} down to 700°C and kept for 100–500 h. Glasses were then examined by the XRD to check whether crystallized phases formed after the heat treatment. The as-treated glasses were cut and ground to bars with nominal dimensions of $15 \times 4 \times 2$ mm^3. The bars were subsequently subjected to the TEC characterization using the dilatometer.

The chemical reactivity between the sealing glass and dense 8YSZ was investigated through heat-treatment experiments at 700°C, where a glass/8YSZ couple, with a glass pellet on the top of an 8YSZ disk, was first heated to 900°C for 30 min to ensure a complete wetting of the glass to the 8YSZ disk. It was then cooled down to 700°C and kept for up to 500 h, after which the glass/8YSZ interface was checked using Field-Emission Scanning Electron Microscopy (FESEM, FEI Quanta 200 FEG, Philips, The Netherlands) and the associated energy dispersive X-ray Spectroscopy (EDS) to reveal the chemical reactivity and any microstructural changes.

Bonding and Sealing Tests

In order to test the sealing capability of the as-developed glass, sealing between two metal plates was performed with using a home-made experimental set-up illustrated in Figure 2-3. The metal was SS410 stainless steel (sealing dimension was 50 mm × 50 mm) with a measured TEC of 12.2×10^{-6} K^{-1}(RT-700°C). The glass was first cut and ground to bars of $25 \times 3 \times 1.2$ mm^3 dimensions. The bars were then adhered to the end plate using epoxy glue, followed by vertically putting the upper plate on the top of the end plate. The assembly was subsequently heated to 770°C with a heating rate of 5 K min^{-1} and kept for 30 min to ensure a good sealing before cooling down to 700°C with a cooling rate of 2 K min^{-1}, after which air was introduced into the inner chamber of the setup to a pressure about 5.5–6.5 kPa above the atmospheric pressure. The heating and cooling profiles are shown in Figure 2-4. The change of the pressure was measured with U-tube pressure gauge using water as the pressure measuring

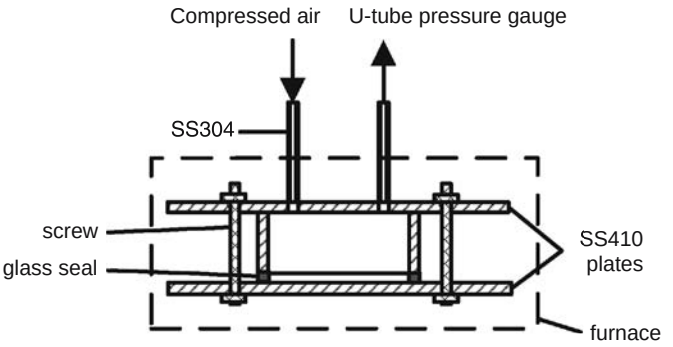

Figure 2-3. Schematic drawing of the leak rate test fixture

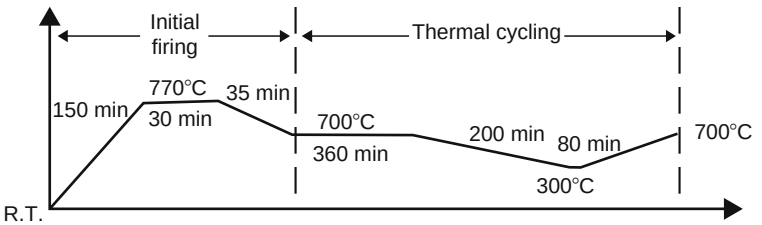

Figure 2-4. Typical temperature profile for initial heat treatment and subsequent thermal cycling tests

media. The leak rate could be calculated based on pressure difference using the ideal gas law as:

$$L = \frac{\mathrm{d}P \times 9.80665 \times V}{8.314 \times T} \times 0.0224, \tag{11}$$

where T is the temperature, V is the volume of the inner chamber and equals to 29.7 cm^3 for the current setup, the dP is the instantaneous pressure drop at a inner–outer pressure difference P, L is the leak rate normalized to the standard state in sccm. The calculated leak rate was further normalized with respect to the leak length (20 cm).

RESULTS AND DISCUSSION

Glass Development

During the initial stage of sealing glass development, we put much effort on the chemical compatibility issue, aiming at developing a sealing glass that could be chemically compatible with 8YSZ. According to the

thermodynamic theory, if 8YSZ is chemically compatible with a glass at high temperatures, 8YSZ must be equilibrium with the glass, which would need the glass saturated with 8YSZ. In other words, in the saturation state, 8YSZ should not react with the glass. So, saturation points of zirconia in various glasses were calculated to predict chemical compatibility of glasses with 8YSZ at high temperatures, using the thermodynamic model established previously. Such simulations started from the system of SiO_2–B_2O_3–Al_2O_3–Li_2O–CaO–ZrO_2, where the ZrO_2 content in the (56–x) SiO_2–23B_2O_3–15Li_2O–7CaO–$x$$ZrO_2$ (wt%) system was increased to see whether ZrO_2 would stay in the liquid phase or in the solid phase to determine the solution limit of ZrO_2 in the glass system. Simulations in this system showed surprisingly good agreement with those experimental results. For example, the saturation point of zirconia in the glass system was calculated to be around 5 wt%. In comparison, it was determined experimentally to be around 7 wt%. Similar good agreement between the calculated results and experimentally determined values was also demonstrated for the saturation point of alumina in a similar system [32], suggesting that the thermodynamic model was reasonably correct.

Since alkali metal oxides like Li_2O has been proven to be too reactive to various SOFC materials at high temperatures, our sealing glass development focused mainly on glasses without alkali metal oxides. Thermodynamic simulations were subsequently focused on the SiO_2–B_2O_3–BaO–La_2O_3–Y_2O_3–ZrO_2 system. Investigations revealed that simulation results were not as good as those of the SiO_2–B_2O_3–Al_2O_3–Li_2O–CaO–ZrO_2 system, due primarily to the lack of sufficient associate species from ZrO_2, Y_2O_3, La_2O_3, and BaO in the thermodynamic model. We shall add more associate species in our future work to make the model more reliable. However, even with this tentative model, thermodynamic simulation could provide very useful information over glass–8YSZ interactions at high temperatures. For example, the reaction behavior of 8YSZ with glasses was largely dependent on glass composition. Thermodynamic simulations predicted that $ZrSiO_4$ and $BaZrO_3$ would be the main resultant phases after 1 mol glass reacts with 1 mol 8YSZ, which was in a good agreement with our experimental results, where the glass in powder form was mixed with 8YSZ powder and heat treated at 800°C for 100 h. Figure 2-5 shows the XRD pattern of the mixture after the heat treatment, which shows clearly the formation of the Ba_2ZrO_4 phase.

We also intended to investigate thermal stability of a glass through thermodynamic simulation. The purpose was to investigate whether it was possible to avoid the formation of some low TEC phases like $ZrSiO_4$ (4.2×10^{-6} K^{-1},100–200°C) [33], celsian phase (2.29×10^{-6} K^{-1} for 20–300°C) and hexacelsian (7.1×10^{-6} K^{-1} for 20–1,000°C) [12], through manipulating the

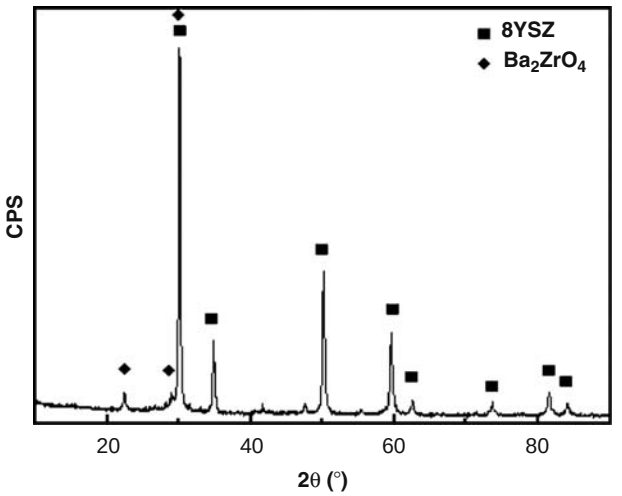

Figure 2-5. XRD pattern of the glass–8YSZ mixture heat treated at 800°C for 100 h in air

glass composition. However, such idea has not been fully realized due to the lack of thermodynamic data for phases like $ZrSiO_4$ and $BaAl_2Si_2O_8$. Nevertheless, our investigations did show that through manipulating the glass composition these low TEC phases could indeed be eliminated, which could significantly improve the thermal stability of the glass. For example, in the glasses containing a high quantity of BaO, $BaAl_2Si_2O_8$ was found to be easily precipitated out from glasses and the successive precipitation of $BaAl_2Si_2O_8$ from these glasses would cause a continuous decrease of TEC value of the glass, which greatly reduces the thermal stability of the glass, as already demonstrated by Sohn et al. [9]. So, the prevention of $BaAl_2Si_2O_8$ formation is crucial for improving thermal stability of sealing glasses containing a high amount of BaO. Our analyses revealed that the formation of $BaAl_2Si_2O_8$ phases could be avoided if the amount of alumina was limited in the SiO_2–B_2O_3–Al_2O_3– CaO–BaO–Y_2O_3–ZrO_2 system. Subsequent experiments confirmed this point, where glasses with different Al_2O_3 contents were heat treated at 800°C for 10–300 h, followed by XRD characterizations to reveal crystalline phase development. As illustrated in Figure 2-6, for glasses containing 10 wt% Al_2O_3, $BaAl_2Si_2O_8$ phases were easily identified after being heat treated for just 10 h at 800°C. The thermal stability of glasses increases with decreasing Al_2O_3 contents in the glass, where no peaks from $BaAl_2Si_2O_8$ phases could be detected by the XRD characterization after being heat treated for 300 h at 800°C when the glass contained only 1 wt% alumina.

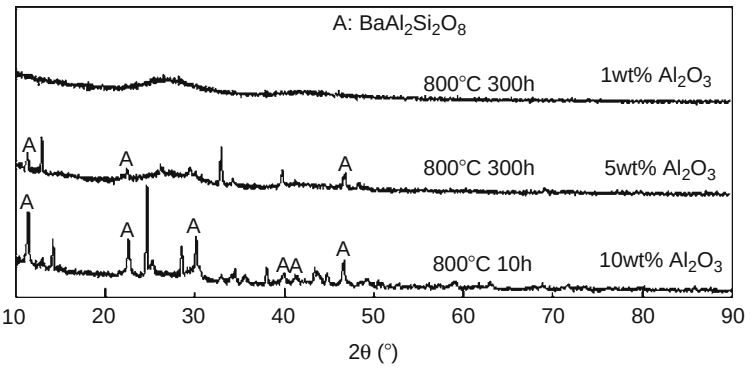

Figure 2-6. XRD patterns of glasses after being heat treated at 800°C for 10–300 h

It should be noted that at the present stage it would be quite difficult to predict complete reaction behaviors for real sealing glass system, using the thermodynamic model previously established. However, the above-mentioned investigations have clearly demonstrated that thermodynamic analyses could provide not only the useful information about various reactions among different materials, but also help to understand glass crystallization behaviors, which could help to find ways to improve sealing glass performances. Further addition of more associate species should make the model more robust for the prediction of various reactions between glasses and other SOFC materials.

After extensive searching in the SiO_2–B_2O_3–Al_2O_3–CaO–BaO–Y_2O_3–ZrO_2 system, a glass with promising properties was successfully developed. The composition of the glass is listed in Table 2-3.

Thermal Properties

Figure 2-7 shows a typical thermal expansion curve for the newly developed glass together with that of 8YSZ, where the TEC value of the glass was calculated to be 9.9×10^{-6} K^{-1} between room temperature (RT) and 631°C (dilatometer determined T_g), very close to the TEC value of 10.0×10^{-6} K^{-1} measured for 8YSZ in the same temperature range. The glass transition temperature is lower than the targeted use temperature (e.g., 700°C), which would be beneficial to thermal stress release at the

Table 2-3. Composition of the newly developed sealing glass

Substance	SiO_2	B_2O_3	BaO	Additives (ZrO_2, Y_2O_3, La_2O_3, ZnO)
wt%	24	20	50	6.0

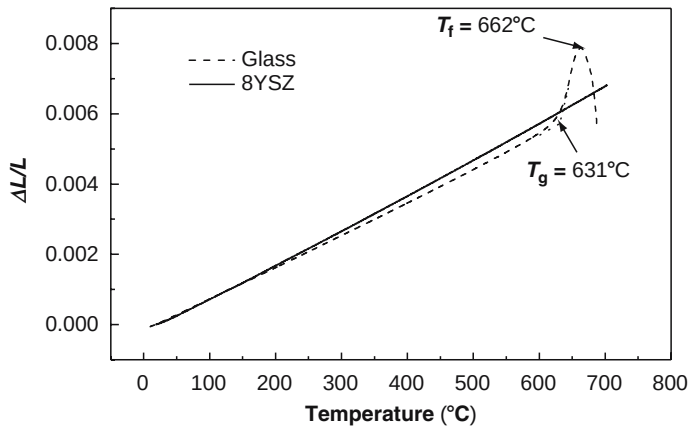

Figure 2-7. Thermal expansion behaviors of a newly developed sealing glass and 8YSZ (10°C min^{-1}, in air)

operating temperature of SOFC since significant stress begin to develop only as the temperature drops below T_g [8].

In order to find the sealing temperature, the wetting behaviors of the newly developed glass on 8YSZ were investigated by observing shape changes of the glass sample on the 8YSZ plate with increased temperature, as illustrated in Figure 2-8. From which, three temperatures 770°C, 810°C and 840°C, corresponding to three characteristic shapes, were determined. At 770°C, the edges of the sample become round. At 810°C, the sample was completely round except the part in contact with the 8YSZ (the ball point temperature), while at 840°C, the shape changed to a hemisphere (called the hemisphere point temperature [34]), and a good wetting between the glass and 8YSZ was achieved with the contact angle less than 90°. Two features could be determined by these observations. Firstly, the glass shows sufficient rigidity at 700°C, which makes it possible to be used as the sealing materials for SOFCs operated at 700°C. Secondly, the sealing temperature can be determined between 810 and 840°C.

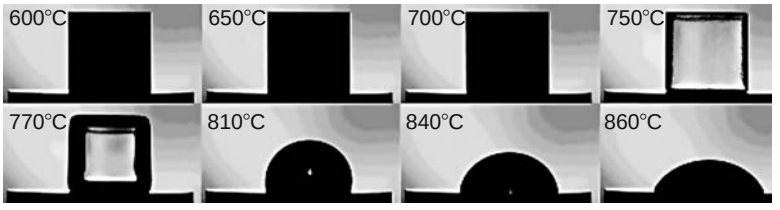

Figure 2-8. Shape change of the glass specimen with increasing temperatures (heating rate 5°C min^{-1})

Thermal Stability

The thermal stability of the newly developed glass was investigated through annealing the glass at 700°C and at 800°C for up to 500 h, after which the TECs were measured and compared with those of the original glass and those reported in literature [9]. Figure 2-9 shows the TEC values against the annealing time. It is seen that after annealing at 800°C for 300 h and at 700°C for 500 h, the TEC change of the glass is less than 2%, which is well within the measuring limit (±1.5%) of the equipment, demonstrating superior thermal stability of the glass. Also, after the annealing tests, no crystalline phases were identified by the XRD characterization and the glass looks completely transparent as demonstrated in Figure 2-10.

Achieving long-term thermal stability is one of the main issues in developing a suitable sealing glass and glass–ceramic for advanced planar SOFC stacks. However, glasses are susceptible to devitrification at high temperatures, which causes significant change of thermal properties. As illustrated in Figure 2-9, the TEC change can be as high as 35% after a similar heat treatment at 800°C for 500 h for the $BaO–Al_2O_3–B_2O_3–SiO_2–La_2O_3–ZrO_2$ glasses reported by Sohn et al. [9]. The present investigation demonstrates, however, that it is possible to develop glasses with superior thermal stability at high temperatures, although further tests are necessary to reveal the long-term thermal stability of the newly developed sealing glass.

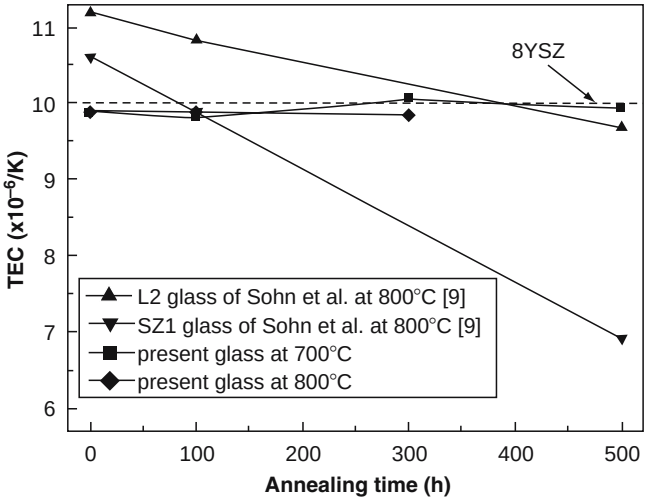

Figure 2-9. Variation of TEC values as a function of annealing time at 700 and 800°C

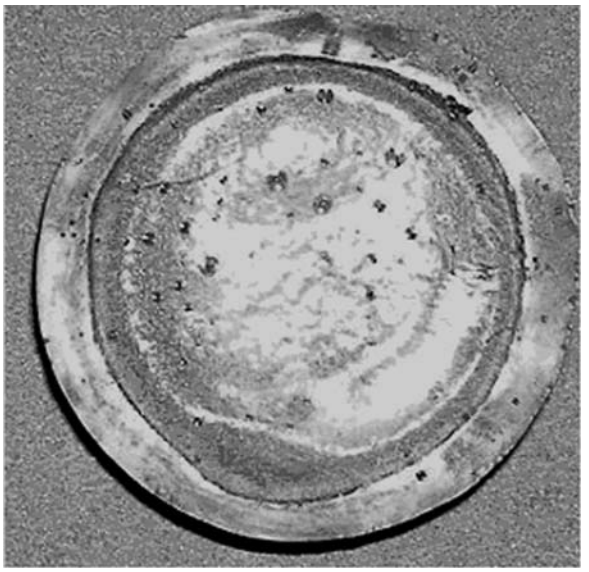

Figure 2-10. Appearance of the glass after being annealed at 700°C for 100 h

Chemical Compatibility with 8YSZ

For SOFC applications, it is quite important to avoid adverse interfacial reactions between sealing materials and the materials to be sealed. The chemical compatibility of the newly developed glass with 8YSZ was therefore examined through heat-treatment experiments at 700°C. Figure 2-11 shows microstructures of the glass/8YSZ interface after the heat-treatment tests, from which it is clear that the glass bonds 8YSZ very well without any micro- and macrocracks. The microstructure shows a clear 8YSZ/glass interface, indicating that interfacial reactions are insignificant after being heat treated with 8YSZ at 700°C for up to 500 h. To further reveal the interfacial interaction, elemental distribution profile was acquired by the EDS line scanning technique and is shown in Figure 2-12. It shows that the concentrations of Zr and Y drop sharply at the interface and the diffusion layer was roughly determined to be 7.6 μm and 8.1 μm after annealing for 100 h and 500 h, respectively, indicating that the interfacial diffusion is limited to a narrow region.

Crystallization Control

Since glasses are thermodynamically unstable, they will eventually crystallize to form glass–ceramics at high temperatures. It is therefore advantageous to control the crystallization process in order to adjust glass

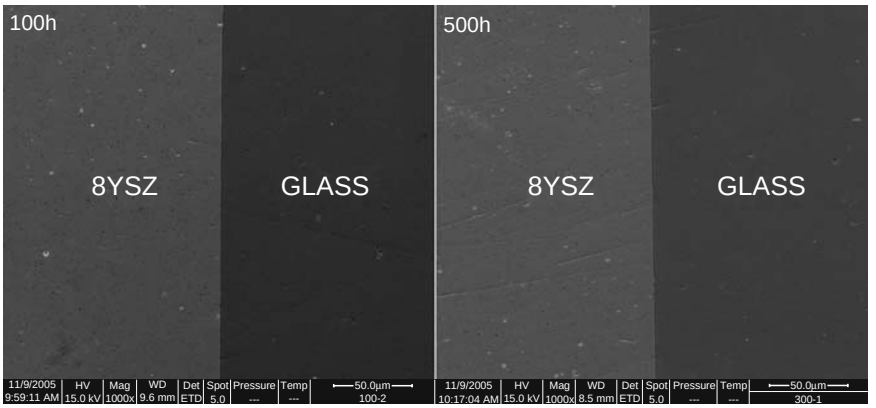

Figure 2-11. Microstructure of the glass/YSZ interface after being heat treated at 700°C for 100 and 500 h

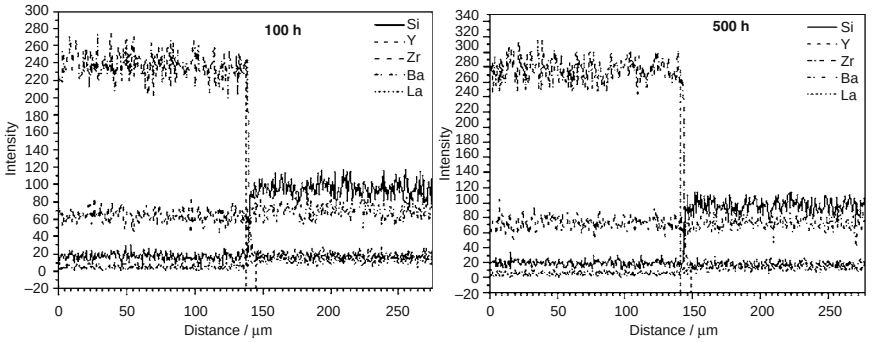

Figure 2-12. EDS line analyses for the glass/YSZ interface heat treated at 700°C for 100 or 500 h

properties. The purposes of the crystallization control include avoiding unwanted phases formation, promoting desirable phases formation, facilitating uniform crystal formation, etc. The crystallization process is usually controlled through manipulating crystallization kinetics (nucleation agents, nucleating conditions, crystallization conditions, etc.).

Our investigations revealed that without a nucleating agent, the newly developed glass is difficult to crystallize. Consequently, various oxides including ZrO_2, TiO_2, Cr_2O_3, P_2O_5 were tried as the nucleating agents for the glass. It was found that the addition of P_2O_5 was quite effective for the crystallization control. The crystallization conditions (e.g., nucleating and crystallization temperatures) were normally determined according to thermal analyses, where it was generally proposed that the nucleation should be performed at a temperature between T_g and 30°C above T_g, while the

crystallization temperature should be around the crystallization temperature (T_c) and 30°C below the liquid temperature (T_{liq}). The DSC curve was thus characterized for the newly developed glass with an addition of 5wt% of P_2O_5, as illustrated in Figure 2-13.

The T_g, T_c, and T_{liq} were determined from Figure 2-13 to be 663°C, 791°, 1061°C, respectively. Accordingly, the nucleating temperature was determined to be 692°C and the crystallization temperature was determined to 820–920°C. Figure 2-14 shows the XRD patterns for glasses after the heat treatment under different conditions. It shows that $Ba_{4.5}La_{4.5}O_{24}P_{1.5}Si_{4.5}$ precipitates out as the main crystalline phase after being heat treated at 820°C for 10 h, while $Ba_3LaO_{12}P_3$ is the main crystalline phase for the heat treatment at 880 and 920°C for 10 h, demonstrating that crystallization behavior could be manipulated through adjusting the crystallization kinetics. It is envisaged that the precipitation of $Ba_3LaO_{12}P_3$ would be better since the glass former (SiO_2) is not precipitated out, so the remaining glass would have a higher SiO_2 content and consequently better stability as compared with the parent glass. The TECs were also characterized for the as-crystallized glass. As illustrated in Figure 2-15, an increase in the TEC was recorded for the glass crystallized at 920°C for 10 h, and the as-crystallized glass and 8YSZ have nearly the same thermal expansion behavior before the glass transition temperature.

Although further detailed investigations are definitely needed to obtain a glass–ceramic sealing material, the above preliminary investigation demonstrated that the properties of the newly developed glass can be well adjusted through the crystallization control process.

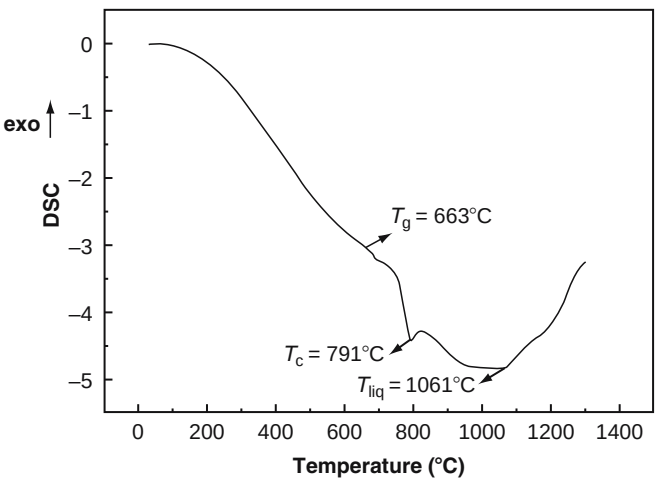

Figure 2-13. DSC curve of the glass with P_2O_5 nucleating agent at a heating rate of 10°C min^{-1} in air

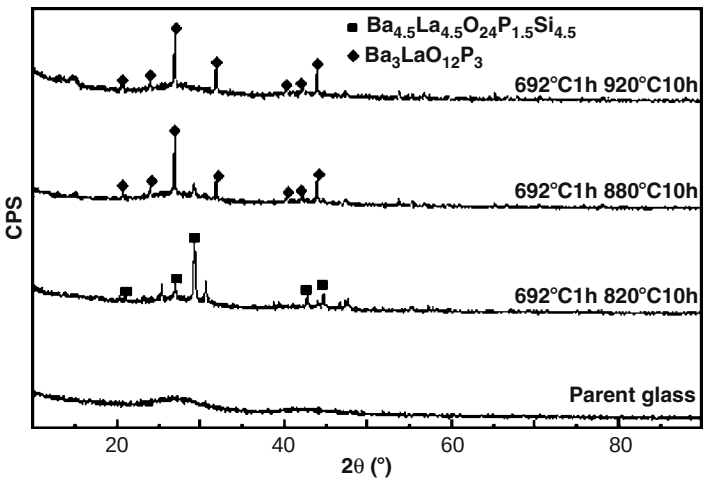

Figure 2-14. XRD of the glass after different heat treatment together with P_2O_5 as the nucleating agent

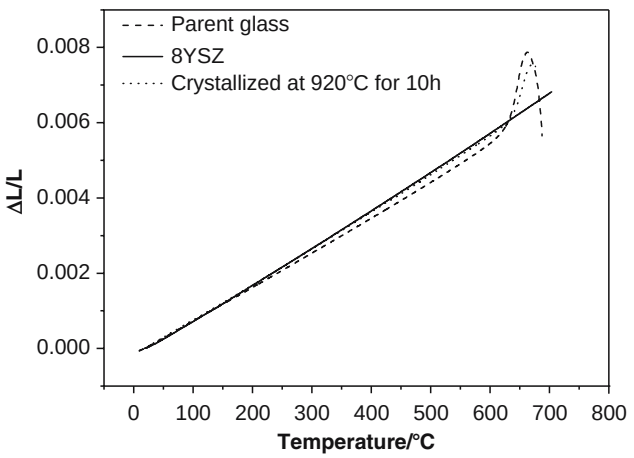

Figure 2-15. Thermal expansion behaviors of parent glass, as-crystallized glass–ceramic and 8YSZ

Sealing Capability

Bonding tests revealed that the sealing temperature was strongly dependent on the load during the sealing process, e.g., without a load, a temperature over 830°C would be necessary to achieve a good wetting and bonding between the glass and 8YSZ or metal interconnect. However, when applying a load of 8.56 kPa (weight of the sealing test fixture), the sealing temperature could be reduced to 770°C. On the other hand, good

sealing cannot be achieved below 750°C, irrespective the load applied. Investigations revealed that bonding strength between the glass and 8YSZ or SS410 stainless steel was quite good, e.g., after intentional breaking the sealing, cracks were actually found to propagate within the glass matrix, not along the glass–metal interface, indicating that the interfacial bonding strength is higher than the strength of the glass.

The sealing capability of the newly developed glass was subsequently tested through measuring the leak rate of air sealed in the chamber shown in Figure 2-3. Before real tests at 700°C, background leak rate was first tested at room temperature using a rubber seal. The background pressure drop with time is illustrated in Figure 2-16, where the figure also reveals that the leak rate is dependent on the pressure difference and it was calculated to be 1.38×10^{-5} sccm cm^{-1} at a pressure difference of 1.4 kPa. Ideally, the leak rate should be zero for a hermetic seal. In reality, the actual low leak rates were limited by the system's background since there were valves and tube connectors in the setup [35].

Figure 2-17 shows the leak rates vs. thermal cycle numbers, where the leak rate of the as-sealed setup is 2.63×10^{-5} sccm cm^{-1}, which is twice as measured background leak rate. Interestingly, the leak rate decreases with increasing the number of thermal cycles. As illustrated in Figure 2-17, after three thermal cycles, the leak rate decreased to 9.76×10^{-6} sccm cm^{-1}, which is even lower than the background leak rate. The reason for this might be due the fact that the background leak rate was measured using a rubber seal at room temperature, which may be different significantly as compared with that of glass seal measured at 700°C.

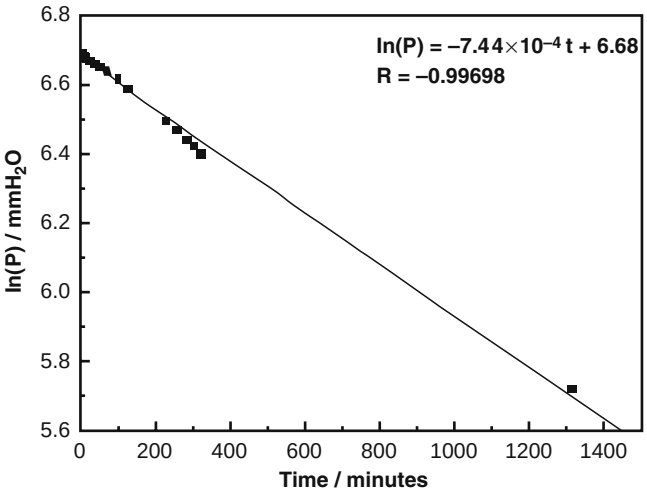

Figure 2-16. Pressure drop of the background leak test for the current test setup

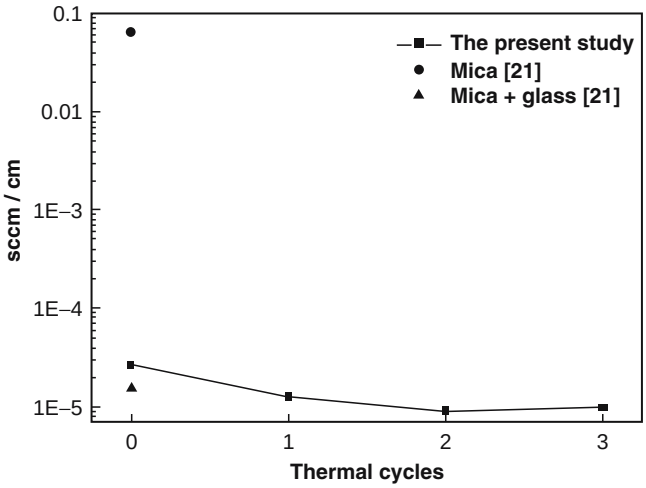

Figure 2-17. Normalized leak rates (sccm cm^{-1}) vs. the number of thermal cycles

The leak rates reported by Chou et al. [21] on mica-based seals were normalized to the pressure of 1.4 kPa and are plotted in Figure 2-17 for comparison. It is clear that the leak rate is nearly the same as reported for the mica–glass composite compressive seals in the literature [21], and it is three orders of magnitudes lower than that of the pure mica compressive seal [21]. The above preliminary sealing tests demonstrated that very good hermetic capability could be achieved for the newly developed sealing glass, together with the capability of withstanding thermal cycles.

CONCLUSIONS

In the present study, a new approach, aiming at quasiquantitative design of sealing glasses, has been proposed. By this method, a glass was developed for SOFCs operated at 700°C. The glass has a thermal expansion coefficient of 9.9×10^{-6} K^{-1}, which is quite close to the value of 10.0 $\times 10^{-6}$ K^{-1} measured for 8YSZ under similar conditions. The sealing glass exhibits superior long-term thermal stability, where after being heat treated for 500 h at 700°C, the change of the TEC value is within the range of equipment error. The glass shows good chemical compatibility with 8YSZ, where no obvious interfacial reaction was detected after being heat treated for 500 h at 700°C together with 8YSZ. Also, the glass properties can be adjusted through the control of crystallization process to obtain a suitable glass–ceramic.

The newly developed glass can wet and bond 8YSZ and SS 410 stainless steel readily above 830°C and it can be effective sealed with 8YSZ and SS410 stainless above 770°C with the applying load of 8.56 kPa. Sealing tests demonstrated that the glass has very good hermetic capability, where the leak rate was measured to be 9.76×10^{-6} sccm cm^{-1}.

The newly developed sealing glass could be a promising candidate for advanced planar SOFC applications.

ACKNOWLEDGEMENTS

The authors would like to acknowledge the financial support from the National Natural Science Foundation of China(Grant No. 20406023).

References

[1] O. Yamamoto, Solid oxide fuel cells: fundamental aspects and prospects, *Electrochimica Acta*, 45 (2000) 2423.
[2] P. Costamagna, A. Selimovic, M.D. Borghi, and G. Agnew, Electrochemical model of the integrated planar solid oxide fuel cell (IP-SOFC), *Chemical Engineering Journal*, 102 (2004) 61.
[3] P. Singh, Nasa, Pacific northwest team on SOFC sealing, *Fuel Cells Bulletin*, 2 (2004) 6.
[4] W. Fergus, Sealants for solid oxide fuel cells, *Journal of Power Sources*, 147 (2005) 46–57.
[5] K.D. Meinhardt, J.D. Vienna, T.R. Armstrong, et al., Glass–ceramic material and method of making, US Patent No. 6430966, August 13, 2002.
[6] P.H. Larsen, C. Bagger, M. Mogensen, et al., *Proceedings of Fourth International Symposium on Solid Oxide Fuel Cells*, eds. M. Dokiya, O. Yamamoto, H. Tagawa and S.C. Singhal The Electrochemcial Society, Pennington, NJ, V95-1, 1995, pp. 69–78.
[7] P.H. Larsen, F.W. Poulsen, and R.W. Berg, The influence of SiO_2 addition to $2MgO–Al_2O_3–3.3P_2O_5$ glass, *Journal of Non-Crystalline Solids,* 244 (1999) 16–24.
[8] K. Ley, M. Krumpelt, R. Kumar, et al., Glass–ceramic sealants for solid oxide fuel cells: Part I. Physical properties, *Journal of Materials Research*, 11 (1996) 1489–1493.
[9] S.B. Sohn, S.Y. Choi, G.H. Kim, et al., Suitable glass–ceramic sealant for planar solid-oxide fuel cells, *Journal of the American Ceramic Society*, 87 (2004) 254–260.
[10] P.H. Larsen and P.F. James, Chemical stability of $MgO/CaO/Cr_2O_3–Al_2O_3–B_2O_3–$phosphate glasses in solid oxide fuel cell environment, *Journal of Materials Science*, 33 (1998) 2499–2507.
[11] Z. Yang, J.W. Stevenson, and K.D. Meinhardt, Chemical interactions of barium–calcium–aluminosilicate-based sealing glasses with oxidation resistant alloys, *Solid State Ionics*, 160 (2003) 213–225.
[12] K. Eichler, G. Solow, P. Otschik, et al., BAS ($BaO–Al_2O_3–SiO_2$)-glasses for high temperature applications, *Journal of the European Ceramic Society*, 19 (1999) 1101–1104.
[13] C. Lara, M.J. Pascual, and A. Duran, Glass-forming ability, sinterability and thermal properties in the systems $RO–BaO–SiO_2$ (R=Mg, Zn), *Journal of Non-Crystalline Solids*, 348 (2004) 149–155.
[14] I.D. Bloom and K.L. Ley. Compliant sealants for solid oxide fuel cells and other ceramics, US Patent No. 5453331, Sept. 26, 1995.

[15] V.A.C. Haanappel, V. Shemet, S.M. Gross, et al., Behaviour of various glass–ceramic sealants with ferritic steels under simulated SOFC stack conditions, *Journal of Power Sources*, 150 (2005) 86–100.
[16] M.C. Tucker, C.P. Jacobson, L.C. De Jonghe, et al., A braze system for sealing metal-supported solid oxide fuel cells, *Journal of Power Sources*, 160(2) (2006) 1049–1057.
[17] K.S. Weil, C.A. Coyle, J.T. Darsell, et al., Effects of thermal cycling and thermal aging on the hermeticity and strength of silver–copper oxide air-brazed seals, *Journal of Power Sources*, 152 (2005) 97–104.
[18] M. Bram, S. Reckers, and P. Drinovac, Characterization and evaluation of compression loaded sealing concepts for SOFC stacks, *Electrochemical Society Proceedings*, 7 (2003) 888–897.
[19] S.P. Simner and J.W. Stevenson, Compressive mica seals for SOFC applications, *Journal of Power Sources*, 102 (2001) 310–316.
[20] Y.S. Chou and J.W. Stevenson, Thermal cycling and degradation mechanisms of compressive mica-based seals for solid oxide fuel cells, *Journal of Power Sources*, 112 (2002) 376–383.
[21] Y.S. Chou, J.W. Stevenson, and L.A. Chick, Novel compressive mica seals with metallic interlayers for solid oxide fuel cell applications, *Journal of the American Ceramic Society*, 86(6) (2003) 1003–1007.
[22] M. Cable, Classical glass technology. *Materials Science and Technology, Vol. 9: Glasses and amorphous materials*, eds. R.W. Cahn, P. Haasen, and E.J. Kramer. VCH, Weinheim, Germany, 1991, pp. 30–31.
[23] T. Lakatos, L.-G. Johansson, and B. Simmingskold, Viscosity temperature relations in the glass systems, *Glass Technology*, 13 (1972) 88–95.
[24] H. Zhang and Q. Zhu, Glass composition prediction using a combined GA-BFGS algorithm, *Computer and Applied Chemistry*, 20 (2003)335–339.
[25] W.B. White, S.M. Johnson, and G.B. Dantzig, Chemical equilibrium in complex mixtures, *The Journal of Chemical Physics*, 28 (1958) 751.
[26] T.M. Besmann and K.E. Spear, Thermochemical modeling of oxide glasses, *Journal of the American Ceramic Society*, 85 (2002) 2887–2894.
[27] A.D. Pelton and M. Blander, Thermodynamic analysis of ordered liquid solutions by a modified quasi-chemical approach-application to silicate slags, *Metallurgical Transactions B*, 17B (1986) 805–815.
[28] A.D. Pelton and P. Wu, Thermodynamic modeling in glass-forming melts, *Journal of Non-Crystalline Solids*, 253 (1999) 178–191.
[29] K.E. Spear, T.M. Besmann, and E.C. Beahm, Thermochemical modeling of glass: application to high-level nuclear waste glass, *MRS Bulletin* 24 (1999) 37–44.
[30] I. Barin, F. Sauert, E. Schultze-rhonhof, et al., *Thermochemical Data of Pure Substance*, Federal Republic of Germany, 1993.
[31] M.W. Chase Jr., C.W. Davies, J.R. Downey Jr., et al., JANAF Thermochemical Tables, 3rd ed. *J. Phys. Chem. Ref. Data*, Vol. 14, Suppl. 1. American Chemical Society, New York, 1985.
[32] Q. Zhu, G. de With, L.J.M.G. Dortmans, et al., Near net-shape fabrication of alumina glass composites, *Journal of the European Ceramic Society*, 25 (2005) 633–638.
[33] I.W. Donald, Preparation, properties and chemistry of glass and glass–ceramic-to-metal seals and coatings, *Journal of Materials Science*, 28 (1993) 2841–2886.
[34] T. Schewickert, R. Sievering, and P. Geasee, Glass–ceramic materials as sealants for SOFC applications, *Materialwiss Werkst*, 33(6) (2002) 363–366.
[35] Y.S. Chou, J.W. Stevenson, and L.A. Chick, Ultra-low leak rate of hybrid compressive mica seals for solid oxide fuel cells, *Journal of Power Sources*, 112 (2002) 130–136.